IJE TRANSACTIONS A: Basics Vol. 26, No. 4, (April 2013) 333-340

International Journal of Engineering

Journal Homepage: www.ije.ir

Performance Evaluation of a High-altitude Launch Technique to Orbit Using Atmospheric Properties

M. R. Taheri [a], A. Soleymani [a], A. Toloei*[a], A. R. Vali [b]

[a] Space Engineering, New Technologies Engineering Faculty, Shahid Beheshti University, Tehran, Iran,
[b] Department of Electrical Engineering, Maleke Ashtar University of Technology, Iran

PAPER INFO

Paper history:
Received 28 April 2012
Received in revised form 23 July 2012
Accepted 18 October 2012

Keywords:
High Altitude Launch
Trajectory Model
Atmospheric Conditions
Performance Evaluation
Near Space
SAFIR-2 Mission

ABSTRACT

The purpose of this paper is to perform the feasibility and performance evaluation of a High-altitude launch technique using high altitude atmospheric properties to near earth orbits. It is suggested in this paper to analyze a different type of launch from a high altitude to the LEO orbit. Two altitudes serve as an initial launch conditions, 20 to 40 km that is evaluated according to the thrust profile variations with respect to the vehicle's payload and under different orbital altitude. the trajectory equations used in the simulation code also take into consideration Spectral and Diffusive reflection model for near space conditions. The methodology is based on the previously mentioned model that calculates the forces affecting a flat plate as it gains altitude. To continue, for validation to problem results, are simulated the mission of SAFIR-2 launch vehicle for it and the output data are compared with the operational phase.

doi: *10.5829/idosi.ije.2013.26.04a.02*

NOMENCLATURE

A	Surface area of plate (m^2)	dp	Momentum (N-m)
β	Angle between velocity vector $\vec{V}$ and unit vector $\hat{q}$	p_{acc}	Coefficient of accommodation
F_C	Centrifugal force (N)	dQ	Energy (W)
$F_{\parallel}$	Force acting in parallel to plate (N)	Φ_T	Thrust angle (deg)
$F_{\perp}$	Force acting perpendicularly to plate (N)	$d\Phi$	Incident particle flux
γ	Adiabatic index	$\hat{\varphi}$	Unit vector along plane around the Earth
h_0	Initial launch altitude (km)	$\hat{r}$	Unit vector along the altitude plane
k	Boltzmann's constant	ρ_a	Density at altitude h (kg/m^3)
M	Vehicle mass (kg)	ρ_m	Average mass density of vehicle (kg/m^3)
Ma	Mach number	σ	Stephan-Boltzmann's constant
m	Particle mass (kg)	θ_i	Incident angle from normal perpendicular to surface (deg)
dn	Number of particles	u	Velocity of particle (m/s)
$\bar{\upsilon}$	Mean velocity of particles (m/s)	W	Weight of vehicle (N)

1. INTRODUCTION

The expensive and risky, the current propulsion transportation system from Earth to space is not of interest by any one. Based on technology from the 1970's, the expense of a trip to space remains in the hundreds of millions of dollars. As mentioned by Randall Parker in his article [1], with a safety record that is still worse than aircraft travel when it was in its thirties. the current space travel technology is in dire need of a new direction for the sake of passenger safety. As well as assurance that expensive payload onboard gets delivered as scheduled safely to their destinations [2, 3]. This research surveys operational parameters of a different type of launch during which a vehicle takes off from a high altitude balloon-based launch system using

* Corresponding Author Email: toloei@sbu.ac.ir (A. Toloei)

atmospheric properties. Though this elongates the travel time, it may possibly reduce the dangers associated with the current propulsion transportation system.

The objective of this paper is to perform the performance evaluation of a high altitude launch technique using high altitude atmospheric properties to an orbit in space. Further, it reviews the forces acting on a body as it travels through the atmosphere's continuum region, while also considering atmospheric conditions at near space altitudes. The developed code recreates these launch conditions while providing information on the forces acting on the body during operation launch phase. It also provides the position and velocity where the vehicle travels at given certain initials conditions. Finally, it presents a summary of the acquired simulation results.

2. BACKGROUND AND TRAJECTORY ELEMENTS

According to doing studies about the Near Space project, the highest elevation an unmanned research air launch system has flown is nearly 52 km. This concept of high altitude balloon-based systems carrying rockets has been around since the 1950's. Unfortunately, due to the unstable nature of balloons, much research still needs to be done in stabilizing such a platform for a spacecraft to launch from Near Space [4].

As mentioned before, the spacecraft in this paper will be launched from an altitude and experience near space atmospheric conditions. The following two subsections will discuss the resulting equations of motion.

2. 1. Launch Trajectory Model The basic trajectory code model describes a flat plate traveling along a plane around the Earth as shown Figure 1. Radius *r* and angle φ represent the vehicle's position in a polar coordinate system. Using unit vectors $\hat{\varphi}$ and $\hat{r}$ associated with this coordinate reference, V_φ and V_r described the velocity along those two vectors. The position of the vehicle can then be related to the velocities as follows.

$$r\frac{d\varphi}{dt} = V_\varphi \qquad \frac{dh}{dt} = V_r \tag{1}$$

Note that *h* represents the altitude [5]. The velocity vector is at an angle β with $\hat{\varphi}$ and can be represented as: $V_\varphi = V\cos\beta,\ V_r = V\sin\beta$

The acting forces on the vehicle are as shown on the right diagram of Figure 1. The vehicle's one weight ($\vec{W}$) and centrifugal force (F_C) are directed along with the $\hat{r}$ vector. The lift force ($\vec{L}$) is shown perpendicular and the drag force ($\vec{D}$) parallel to velocity $\vec{V}$. The thrust vector ($\vec{T}$) is at angle ϕ_T with velocity $\vec{V}$. So, the equations of motion of the vehicle become:

$$\begin{cases} M\dfrac{dV_\varphi}{dt} = T\cos(\phi_T+\beta) - D\cos\beta - L\sin\beta \\ M\dfrac{dV_r}{dt} = T\sin(\phi_T+\beta) + L\cos\beta - D\sin\beta + M\dfrac{V_\varphi^{\,2}}{r} - Mg \end{cases} \tag{2}$$

Within the position coordinate system, another coordinate system must be defined. Consider a flat plate at angle of attack α. Unit vectors $\parallel$ and $\perp$ are parallel and perpendicular to the plate respectively as shown in the Figure 2.

Along these unit vectors, forces $F_\parallel$ and $F_\perp$ are related to lift and drag forces as follows [6]:

$$\begin{cases} L = F_\perp\cos\alpha - F\sin\alpha \\ D = F_\perp\sin\alpha + F\cos\alpha \end{cases} \tag{3}$$

Note that the drag force acts in the opposite direction from the velocity.

Substituting Equation (3) into (2), the equations of motion are represented by:

$$\begin{cases} M\dfrac{dV_\varphi}{dt} = T\cos(\phi_T+\beta) - F_\perp\sin(\alpha+\beta) \\ \qquad - F\cos(\alpha+\beta) \\ M\dfrac{dV_r}{dt} = T\sin(\phi_T+\beta) + F_\perp\cos(\alpha+\beta) - F\sin(\alpha+\beta) \\ \qquad + \mathrm{M}\dfrac{V_\varphi^{\,2}}{r} - Mg \end{cases} \tag{4}$$

By assuming certain initial conditions at time t = 0, the next velocity components and therefore angle β can be calculated for the next time step using the Equation (4). The following position of the vehicle is recalculated using Equation (1). The altitude during one time step helps compute the air density and aerodynamic forces acting on the vehicle for the following step.

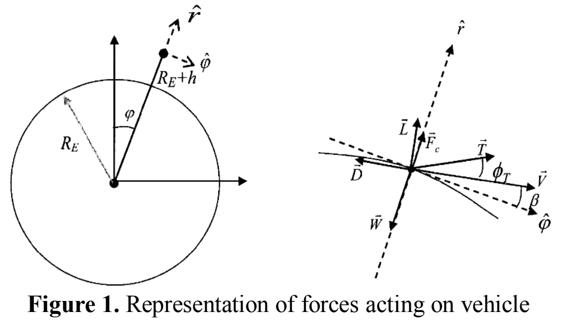

Figure 1. Representation of forces acting on vehicle

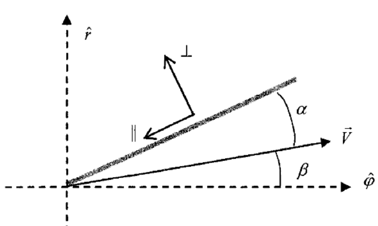

Figure 2. Representation offers acting on plate while at angle α

Though the thrust angle is initially assumed, there are 3 thrust angles cases that must be considered. First case being that $\Phi_T = 0$ and $\vec{T}$ is always along $\vec{V}$. The second scenario is where $\Phi_T = \alpha$ and $\vec{T}$ is along the chord length. The final case is where $\Phi_T = -\beta$ and $\vec{T}$ is always along $\hat{\varphi}$. Since the aerodynamic forces are proportional to the vehicle's surface area (A), and dynamic pressure (ρV^2), we divide both sides of Equation (4) by the vehicle mass to get:

$$\begin{cases} \dfrac{dV_\varphi}{dt} = \dfrac{T}{W} g\cos(\phi_T + \beta) - \dfrac{F_\perp}{M}\sin(\alpha+\beta) - \dfrac{F}{M}\cos(\alpha+\beta) \\ \dfrac{dV_r}{dt} = \dfrac{T}{W} g\sin(\phi_T + \beta) + \dfrac{F_\perp}{M}\cos(\alpha+\beta) - \dfrac{F}{M}\sin(\alpha+\beta) \\ \qquad + \dfrac{{V_\varphi}^2}{r} - g \end{cases} \tag{5}$$

2. 2. Trajectory Model in Near Space

Near space is considered to lie between 20-100 km in altitude. It's a range of very low density. As this altitude is part of the trajectory presented in this research, the forces acting on the vehicle traveling across that altitude also need to be presented [7, 8].

Consider the following scenario where a flux of incident particles reflects off a surface at an angle θ_i from the normal. The thermal spreading of these particles can be considered negligible, and angle α is the angle of attack from the surface. The unit area dA on the wall onto which the particles hit project an area $dA\cos\theta_i$, as shown in Figure 3 [9]. The flux of particles through this area can be represented as follows [10]:

$$d\Phi = n.u.dA\cos\theta_i \tag{6}$$

For the case of specular reflection (Figure 4), the particle bounces perfectly from the surface at the same angle it arrived at while fully conserving its energy [9]. The momentum and energy transferred to the surface is respectively [10]:

$$\begin{cases} dp_\perp = 2mu\cos\theta_i \\ dp = 0 \\ dQ = 0 \end{cases} \tag{7}$$

During diffusive reflection, the particles reflect according to Maxwellian distribution. This occurs at material temperature T_m in the half-space of $0 < \theta < \pi/2$. The momentum absorbed can be represented by [9]:

$$\begin{cases} dp_\perp = m(u\cos\theta_i + \bar{\upsilon}) \\ dp = mu\sin\theta_i \end{cases} \tag{8}$$

where, the mean velocity, $\bar{\upsilon}$ at the material temperature T_m [11]:

$$\bar{\upsilon} = \left(\frac{kT_m}{2\pi m}\right)^{0.5} \tag{9}$$

By multiplying the particle flux with the momentum equations, the tangential and normal forces projected on the surface are found and shown in the follow equations [5].

$$\begin{aligned} &Specular \begin{cases} dF_\perp = 2\rho u^2 dA\cos^2\theta_i \\ dF = 0 \end{cases} \\ &Diffuse \begin{cases} dF_\perp = \rho u dA\cos\theta_i \left(u\cos\theta_i + \bar{\upsilon}\right) \\ dF = \rho u^2 dA\cos\theta_i \sin\theta_i \end{cases} \end{aligned} \tag{10}$$

Translating them on to the Cartesian coordinate system, the Equation (10) becomes:

$$\begin{cases} dF_x = -dF_\perp \sin\alpha - dF\cos\alpha \\ dF_y = dF_\perp \cos\alpha - dF\sin\alpha \end{cases} \tag{11}$$

The relationship between the unit vectors∥and ⊥, and the x-y-coordinate system is shown in Figure 2. The forces per unit area are then shown in the follow equations.

$$\begin{aligned} &Specular \begin{cases} df_x = -2\rho u^2 \sin^3\alpha \\ df_y = 2\rho u^2 \sin^2\alpha\cos\alpha \end{cases} \\ &Diffuse \begin{cases} df_x = -\rho u^2 \sin\alpha - \bar{\upsilon}.\rho u\sin^2\alpha \\ df_y = \bar{\upsilon}.\rho u\sin\alpha\cos\alpha \end{cases} \end{aligned} \tag{12}$$

The coefficient of accommodation p_{acc} represents the likelihood the particles will behave more according to a perfect diffuse model than a perfect reflective model. The p_{acc} value of unity would be considered a perfect diffusive reflection. For simplicity, we assumed this probability to be a constant, though it usually depends on surface conditions, particle energy, incident angle, and other factors [12]. For our case, p_{acc} was assumed to be 0.1 due to the high temperatures the plate was expected to experience, as well as the cleanliness and smoothness of the plate's surface assumed [10].

Each particle transfers energy onto the wall in the amount of $u^2/2$. Meanwhile, the energy lost by the wall when reflecting a particle is the average energy are shown by equation in article [13]. Finally, the wall was assumed to behave like a black body. The resulting equations for the forces and energy transferred per unit area are:

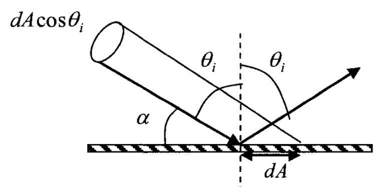

Figure 3. Reflection of incident particles on surface

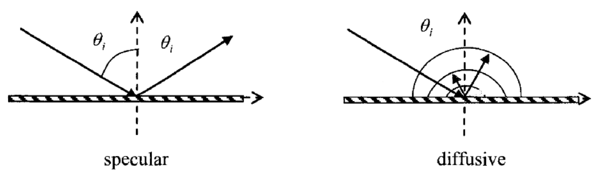

Figure 4. Specular and diffuse reflection

$$\begin{cases} df_x = -\rho u^2 \left[2(1-P_{acc})\sin^3\alpha + P_{acc}\sin\alpha + P_{acc}\sin^2\alpha.\dfrac{\upsilon}{u} \right] \\ df_y = \rho u^2 \left[2(1-P_{acc})\sin^2\alpha\cos\alpha + P_{acc}\sin\alpha\cos\alpha.\dfrac{\upsilon}{u} \right] \\ dq = \rho u \sin\alpha.\dfrac{u^2}{2} - \rho u.P_{acc}.\sin\alpha\left(\dfrac{3kT_m}{4m}\right) - \sigma T_m{}^4 \end{cases} \tag{13}$$

By including thrust, gravity, and centrifugal force that contributed to vehicle's dynamics, the equations become [10]:

$$\begin{cases} M\dfrac{du}{dt} = T_x - A\rho u^2\left[2(1-P_{acc})\sin^3\alpha + P_{acc}\sin\alpha + \right. \\ \qquad \left. P_{acc}\sin^2\alpha.\dfrac{\upsilon}{u}\right] \\ M\dfrac{dv}{dt} = T_y + M\dfrac{u^2}{R_E + h} - Mg + \\ \quad A\rho u^2\left[2(1-P_{acc})\sin^2\alpha\cos\alpha + P_{acc}\sin\alpha\cos\alpha.\dfrac{\upsilon}{u}\right] \end{cases} \tag{14}$$

The forces can be normalized by the weight, and using an average area mass density (ρ_m) for the vehicle:

$$\begin{cases} \dfrac{du}{dt} = \dfrac{T_x}{W}g - \dfrac{\rho_a}{\rho_m}u^2\left[2(1-P_{acc})\sin^3\alpha + \right. \\ \qquad \left. P_{acc}\sin\alpha + P_{acc}\sin^2\alpha.\dfrac{\upsilon}{u}\right] \\ \dfrac{dv}{dt} = \dfrac{T_y}{W}g + \dfrac{u^2}{R_E + h} - g + \\ \qquad \dfrac{\rho_a}{\rho_m}u^2\left[2(1-P_{acc})\sin^2\alpha\cos\alpha + P_{acc}\sin\alpha\cos\alpha.\dfrac{\upsilon}{u}\right] \end{cases} \tag{15}$$

Recall that, $W = Mg$, $\rho_a(h) = \rho_0\exp(-h/h_0)$, $dh/dt = \upsilon$.

In addition to the previous equations, the code calculates the Mach number at every point of the trajectory. The following equation was used to find the speed of sound [14]:

$$a = \sqrt{\gamma P/\rho} \tag{16}$$

where, we used the adiabatic index, $\gamma = 1.4$. p represents pressure, and ρ is the density of air.

3. METHODOLOGY

The launch conditions needed to be simulated in varying high altitude environments. This was achieved using the MATLAB software that is now so commonly used in the aerospace and many other industries. The code developed is based on the previously mentioned model that calculates the forces affecting a flat plate as it gains altitude. It takes into consideration air density changes with altitude, angles of attack (α), payload, initial altitudes of launch (h_0), and orbital altitude (h_F). The equations used in this code also take into consideration spectral and diffusive reflection for near space conditions. By adding a few computation boundaries such as achieving desired orbital velocity and altitude, is completed simulation process.

Two modes serve as the initial launch locations, 20 and 40 km with under of 10 AOA (angle of attack) for SAFIR-2 launch vehicle mission. The consideration and initial condition for different modes are shown in Tables 1 and 2. These are altitudes through which current high altitude balloon-based launch system are able to achieve. Because the code supplies information on altitude, distance, density, velocity, forces and Mach numbers at every point of the launch trajectory, a parametric study was possible between all the variables. The parametric modes performed included trade studies between the different variables, pitch angle (θ) and drag coefficients (C_x), altitude (H), and vehicle velocities in the x-y-direction at varying angles of attack, pressure (P), thrust vector (P_t) and density (R_0), as to analyze which scenario resulted in the best launch. The parametric modes also helped to determine whether the code was giving valid results.

TABLE 1. Simulation Initial Conditions for 20 km

Mode No.	Payload (kg)	h_F (km)	Altitude (h_0), km	Angle of attack (α), deg
SAFIR-2	27	240	0	0
(1)	27	300	20	10
(2)	180	240	20	10

TABLE 2. Simulation Initial Conditions for 40 km

Mode No.	Payload (kg)	h_F (km)	Altitude (h_0), km	Angle of attack (α), deg
SAFIR-2	27	240	0	0
(3)	27	385	40	10
(4)	330	240	40	10

4. SIMULATION RESULTS AND DISCUSSION

The following texts show the results achieved with the developed code. Table 3 includes the scenarios considered under SAFIR-2 mission specifications. Simulation results are derived for each set of defined modes with respect to performance parameters.

Therefore, we can increase payload to 180 kg with launching from 20 km, 10 AOA and orbital altitude 240 km (Table 1). We can increase orbital altitude to 300 km with launching from 20 km and 10 AOA with supposed payload 27 kg.

In addition, we can increase payload 330 kg with launching from 40 km, 10 AOA and orbital altitude 240 km (Table 2). We can increase orbital altitude to 385 km with launching from 40 km and 10 AOA with supposed payload 27 kg.

Now, by comparative simulation, results in 20 and 40 km altitude are shown in following Figures 5-11.

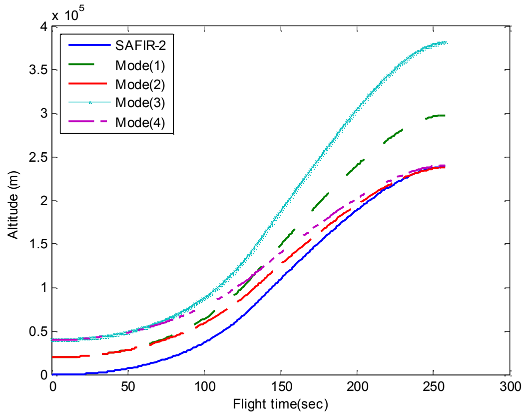

Figure 5. Launch vehicle altitude vs. flight time

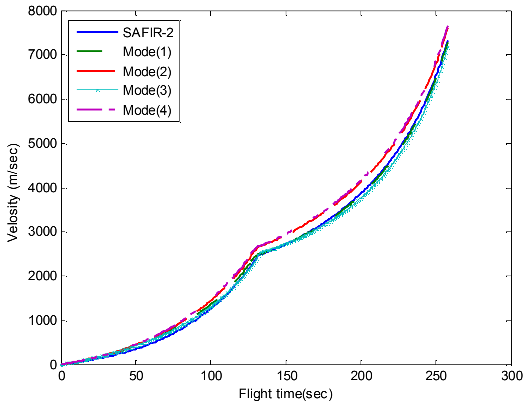

Figure 6. Launch vehicle velocity vs. flight time

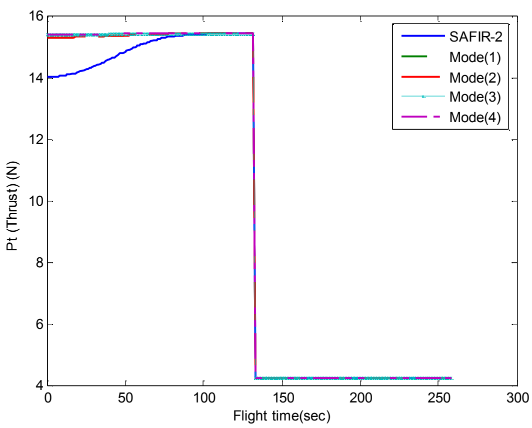

Figure 7. Launch vehicle thrust vector vs. flight time

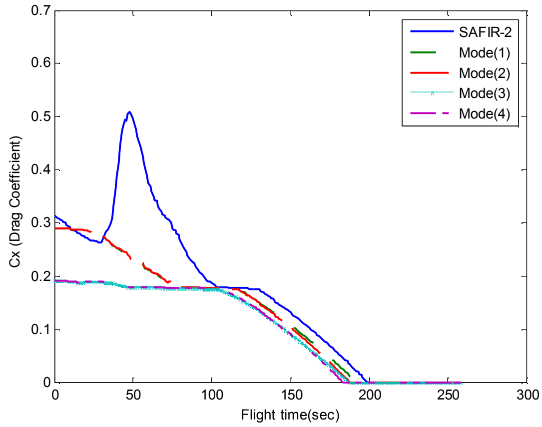

Figure 8. Launch vehicle drag coefficient (C_X) vs. time

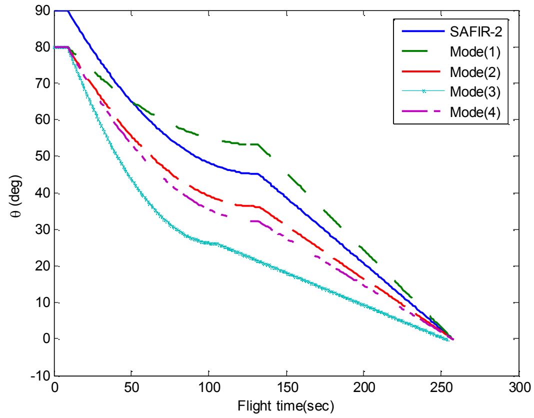

Figure 9. Launch vehicle Pitch angle (θ) vs. flight time

TABLE 3. SAFIR-2 Launch Vehicle Specification

Parameter	stage I	stage II
Dimensions		
Length (m)	17.20	3.2
Diameter (m)	1.25	1.25
Mass		
Propellant Mass (kg)	20,000	4,000
Gross Mass (kg)	2,1978	4,706
Propellant Mass Fraction	0.91	0.85
Propulsion		
Average Thrust (KN) Vacuum	361.2	83.4
I_{SP} *(sec)- Vacuum*	280	298
Mission		
Launch Site: Semnan, Iran (35.57 deg. N Latitude)		
Payload (kg)	*Attitude (km)*	*INCL(deg)*
27	240	55.71 LEO

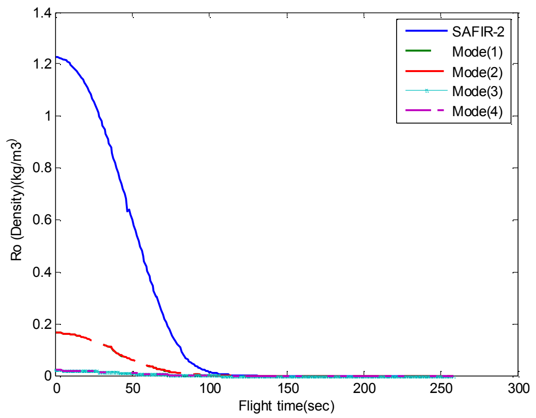

Figure 10. Launch vehicle density (R_0) vs. flight time

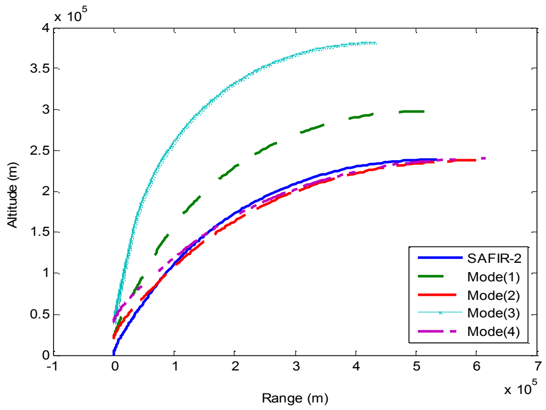

Figure 11. Launch vehicle altitude (*Y*) vs. range (*X*)

TABLE 4. Developed performance percent of SAFIR-2 launch vehicle mission

Mode	h_0 (km)	(α) deg	Payload (kg)	h_f (km)	Increased payload percent (%)	Increased orbital altitude percent (%)
SAFIR-2	0	0	27	240	-----	-----
(1)	20	10	180	240	566	-----
(2)	20	10	27	300	-----	25
(3)	40	10	330	240	1122	-----
(4)	40	10	27	385	-----	60

Figure 5 shows that with an increase in initial altitude, mass of payload or orbital altitude can be increased considerably under same flight time. The major advantage of this technique is shown in Figure 8-10. Because of using the standard atmospheric model and specular and diffuse reflection in basic equation of simulation code, drag coefficient and air density are improved significantly. So, results indicate with a same orbital altitude can increase mass of payload significantly. Furthermore, with a same mass of payload, orbital altitude can be increased in same period of flight time. The major achievement in the innovation and space launch systems is considered.

The developed results for SAFIR-2 mission are shown in Table 4. This table shows the difference between initial height of launch and to surface height. The benefits of using this launch technique for initial altitude is more which makes us appear.

5. CONCLUSION

When comparing all four modes, the first distinct difference was the wider range of angles of attack that the plate could be flown at when launching from the higher altitude of h_0 =40 km.

In general, all the flight trajectories remained smoothest at higher *T/W* ratio. It was also observed that at α =10° results were not favorable at low *T/W* ratios but improved with larger thrust values. When comparing only the simulation results within one initial altitude, the higher the *T/W* ratio, the earlier of the supposed orbital alttitude was achieved.

Therfore, the obtained simulation results for each of four modes indicated that for h_0 =40 km, increased percent of payload and orbital alttitde is more desirable. Thus, this technique can be suitable in development and improvement of the next generation launch system missions.

6. REFERENCES

1. Parker, R., "Aircraft and Space Shuttle Accident Rates", ***Future Pundit***, (2008)
2. Nigro, N., Yang, J., Elkouh, A. and Hinton, D., "Generalized math model for simulation of high-altitude balloon systems", ***Journal of Aircraft***, Vol. 22, No. 8, (1985), 697-704.
3. Kandis, M., Witkowski, A., Machalick, W. and Klein, E., "Energy Modulators for Recovery of High Altitude Balloon Payloads", ***AIAA Balloon Systems Conference***, (2009).
4. Wanagas, J. D. and Gizinski III, S. J., "Small satellite delivery using a balloon-based launch system", in AIAA 14th International Communication Satellite Systems Conference and Exhibit. Vol. 1, (1992).
5. Sarigul-Klijn, N., Sarigul-Klijn, M. and Noel, C., "Air-launching earth to orbit: effects of launch conditions and vehicle aerodynamics", ***Journal of Spacecraft and Rockets***, Vol. 42, (2005).
6. Anderson, J. D., *JR*,"Introduction to Flight", Mc Graw-Hill International Editions, Aerospace Science Series, (1995)
7. Browning, W. M., Olson, D. S. and Keenan, D. E., "High-altitude balloon experiment", in Aerospace/Defense Sensing and Controls, International Society for Optics and Photonics, (1998), 28-36.

8. Runnels, S. R., Smith, M. S. and Fairbrother, D. A., "High-altitude balloon thermal trajectory analysis database system", ***AIAA 3rd Annual Aviation Technology***, (2003).

9. Potter, J. L., "Rarefied gas dynamics, Wiley Online Library, (2007).

10. Loeb, L. B., "The kinetic theory of gases", Dover Publications, (2004).

11. Collie, C., "Kinetic theory and entropy", Longman, (1982).

12. Shukla, P. K. and Mamun, A., "Introduction to dusty plasma physics", Taylor & Francis, Vol. 10, (2001).

13. Anderson, J. D., "Hypersonic and high temperature gas dynamics", ***AIAA***, (2000).

14. John, D. A. and Anderson, J., "Fundamentals of aerodynamics"., Mc Graw Hill, USA. (1991).

Performance Evaluation of a High-altitude Launch Technique to Orbit Using Atmospheric Properties

M. R. Taheri [a], A. Soleymani [a], A. Toloei [a], A. R. Vali [b]

[a] *Space Engineering, New Technologies Engineering Faculty, Shahid Beheshti University, Tehran, Iran,*
[b] *Department of Electrical Engineering, Maleke Ashtar University of Technology, Iran*

PAPER INFO

Paper history:
Received 28 April 2012
Received in revised form 23 July 2012
Accepted 18 October 2012

Keywords:
High Altitude Launch
Trajectory Model
Atmospheric Conditions
Performance Evaluation
Near Space
SAFIR-2 Mission

چکیده

در این مقاله هدف امکان‌سنجی و ارزیابی عملکرد تکنیک پرتاب یک وسیله فضایی از یک ارتفاع خاص جهت استقرار در مدار نزدیک به زمین می‌باشد. در این مقاله پیشنهاد شده‌است که نوع متفاوتی از پرتاب از یک ارتفاع زیاد به یک مدار ارتفاع پایین بررسی و تحلیل شود. در این فرآیند شرایط اولیه پرتاب ارتفاع بالا وسیله مطابق با مطالعات انجام‌گرفته، در نرخ ارتفاع ۲۰ تا ۴۰ کیلومتری بوده که بر حسب تغییرات پروفیل تراست به وزن محموله و تحت ارتفاع مداری مختلف ارزیابی شده است. به دلیل قرارگیری شرایط پرتاب در محدوده فضای مجاور و تحت تاثیر نفوذ اتمسفر زمین، معادلات حاکم بر مسیر حرکت پروازی برای دو مدل انعکاس نفوذی و طیفی شبیه‌سازی و تعیین گردیده است. به منظور کاهش اثر اغتشاشات فضای مجاور در روند حل مسئله، مدل پرتابی به صورت یک صفحه تخت در نظرگرفته شده که در نهایت امر با افزودن شرایط انتهایی تزریق مدار هدف برای محموله موردنظر، فرآیند شبیه‌سازی تکمیل می‌گردد. در ادامه جهت اعتبارسنجی نتایج مسئله، مأموریت ماهواره‌بر سفیر-۲ شبیه‌سازی و داده‌های خروجی با فاز عملیاتی مقایسه شده است.

doi: *10.5829/idosi.ije.2013.26.04a.02*